The Difference of Serum Protein Transport between Echinosides and Verbascoside

[1]Ming Guo, [1]Xiaoxue Zhao, [3]Peter. E. Brodelius, [1]Ling Fang, [2]Zhihong Sun* and [1]Rui Wang
[1]*School of Science, Zhejiang Agricultural & Forestry University, Lin'an 311300, China.*
[2]*School of Forestry and Bio-technology, Zhejiang Agricultural and Forestry University, Lin'an, Zhejiang 311300, China.*
[3]*Department of Chemistry and Biomedical Sciences, Linnaeus University, 391 82 Kalmar, Sweden.*
guoming@zafu.edu.cn*

(Received on 22nd January 2019, accepted in revised form 27th January 2020)

Summary: Verbascoside (VER) is the enzymatic hydrolysis product of echinacoside (ECH). The molecular structures of ECH and VER have different glucosyl groups so they bind to serum albumin in different ways, resulting in different pharmacological actions. In this report, we have examined the binding characteristics between human serum albumin (HSA) and ECH/VER by molecular modeling and spectroscopic approaches. Molecular modeling revealed that VER bound to HSA mainly through hydrogen bonds, van der Waals forces and hydrophobic forces. The spectroscopic results showed that the interactions between HSA and VER/ECH involved a static binding process, and the bonding strength of the VER-HSA complex was stronger than that of the ECH-HSA complex. The value of the binding distances (*r*) was low, which indicated the occurrence of energy transfer. The reaction conformational pattern of HSA-VER and HSA-ECH gave a "two-state model" based on fluorescent phase diagram analysis. According to the thermodynamic model, the main forces between interaction of VER and HSA were hydrogen bonds and van der Waals forces, whereas the interaction between ECH and HSA was hydrophobic force. The fluorescence polarization analysis demonstrated that the interaction between HSA and VER or ECH generated a non-covalent complex. Compared with ECH, VER was more likely to bind with HSA because of its smaller molecular size and low polarity. The results of the spectral analysis concurred with the molecular modeling data, which provides a helpful reference for the study of the molecular reaction mechanism of VER/ECH binding to HSA.

Keywords: Verbascoside, Echinacosid, Serum, Albumin, Spectrum, Experiment, Molecular modeling.

Introduction

Verbascoside (VER) with the formula $C_{29}H_{36}O_{15}$ (molecular formula shown in Fig l) is also known as acteoside. It is a caffeoyl phenylethanoid glycoside. VER is found in the leaves of Dihuang (*Rehmannia glutinosa*), Cistanche (*Cistanche deserticola* and *C. tubulosa*), and many other plants [2]. VER has a significant therapeutic effect on the nervous and immune systems, especially with respect to age-related (Alzheimer's disease) and autoimmune diseases (Chronic nephritis) [4]. Echinacoside (ECH) with the formula $C_{35}H_{46}O_{20}$ (shown in Fig 1) is also known as sea urchin glycoside or echinacea glycoside. It is an active ingredient of cistanche, a traditional Chinese medicine. ECH has significant neuroprotective effects as an antioxidant. ECH also has other health benefits, including anti-neuronal apoptosis, liver protection, anti-inflammatory, anti-tumor, anti-aging, promotion of vasodilation, promotion of tissue healing, and improvement of immunity adjustment [14, 27, 24].

VER and ECH are phenethyl alcohol substances. Research on intestinal bacteria metabolism has shown that ECH, which is the main component of phenethyl alcohol compounds, is converted to VER by microbial enzymatic activities in the large intestine. In the industrial production process, ECH is hydrolyzed to VER by the industrial biocatalyst β-glucosidase (Fig 1). The highly active VER can be extracted, purified, concentrated and dried [1]. Although VER and ECH have similar structures and efficacies, VER is a molecule with low polarity, thereby providing good absorption rate and specific pharmacological activity during the process of drug absorption. The specific pharmacological activity studies on ECH and VER, there is few researches have been carried out [34, 35, 36, 37], which prompt the exploration of interactions between ECH/VER and biomacromolecules.

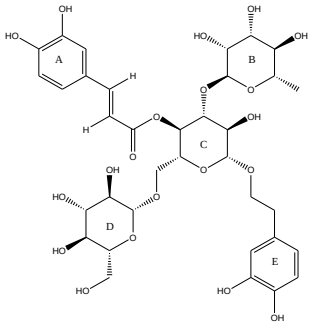

Fig. 1: The chemical structure of Echinacoside.

*To whom all correspondence should be addressed.

The pharmaceutical properties of ECH and VER render it to be absorbed by accumulating, potentially causing interactions with plasma proteins in blood. The transportation, distribution and metabolic processes of ECH/VER are highly dependent on their binding with high abundance transport protein in human plasma--human serum albumin(HSA) [22]. As the most abundant protein in plasma, HSA plays an important role in transport and storing of endogenous metabolites and as well as exogenous drug molecules [17, 9]. Compared with other proteins, HSA is a relatively complex macromolecule with great solubility. HSA has good stability and high affinity towards various ligands, and it can be easily purified in large quantities. In addition, the tertiary structure of HSA is known. This makes it an ideal protein model in the study of interactions between drugs and protein molecules. The main function of HSA is to transport various exogenous and endogenous molecular carrier proteins. HSA interacts with ligands and other proteins and is a key regulator of intercellular flux. HSA is 67 kDa, it's a single polypeptide chain that consists of 585 amino acids [26, 13], there are three helical domains (I, II, III) with similar structure, each helical domain consists of A and B subdomains. HSA usually has two binding chambers in subdomain IIA and IIIA (called Sudlow site I and Sudlow site II, respectively) [22]. The amino acid sequence of HSA contains 35 cysteine residues [11, 16], which form 17 disulfide bonds leaving a single free cysteine residue. Eight pairs of these disulfide bonds form cross-disulfides bonds by crossing two disulfide bonds, and only the one near the N-terminus is not participating in a disulfide bond. HSA contains 18 tyrosine residues, one tryptophan residue at position 214, one aspartic acid residue at the N terminal, and one leucine residue at the C-terminal. The concentration of HSA accounted for 60% of total plasma protein. It transports fatty acids, bile pigments, amino acids, steroids, metal ions, and many therapeutic molecules in body fluids, while maintaining normal osmotic pressure. Drugs binding may affect the conformation and biological function of HSA, and may lead to the biological changes. The binding model between ligands and serum protein may be a useful way to characterize their bioaccumulative potential and bioavailability *in vivo*, therefore, the dynamic interactions between ECH/VER and HSA need to be fully elucidated, which is of significance for evaluating the bioavailability *in vivo*. By exploring the interactions between ECH/VER and HSA under simulating *in vivo*, we do not only obtain pharmacodynamic information about ECH/VER and elucidate the delivery mechanism of ECH/VER, but we also provide a theoretical reference for further ECH/VER analyses. But, there is few such studies have been carried out to study the interaction between ECH/VER and HSA at the atomic level.

The molecular interaction mechanisms of ECH/VCR with HSA were deciphered by spectroscopy and molecular docking at the atomic level.The binding reaction constants, thermodynamic parameters and the impact of drugs on protein conformation were obtained from the spectral data. hermodynamic parameters and the impact of drugs on protein conformation were obtained from the spectral data. Molecular dockings were further carried out to provide atomic insight into the repositioning of different molecules between ECH/VER and HSA. Meanwhile, the combination details of visualization are also consistent with the experimental studies. As far as we know, this is the first time to study the interaction of VER/ECH and HSA *in vitro* and *in silico* [22]. The interaction mechanism between VER/ECH and HSA at the molecular level is presented, thereby providing an important reference for the analysis of the pharmacodynamic mechanisms of VER and ECH.

Experimental

Instruments and reagents

Human serum albumin (HSA, ≥ 98%), verbascoside (VER, 96%), echinacoside (ECH, ≥ 98%) and Tris (GR) were obtained from Shanghai Huamei Bio-Engineering Company. Other reagents were all analytical grade. All aqueous solutions were prepared with distilled water. The Tris-HCl buffer solution was prepared at a concentration of 0.1 mol/L, pH = 7.4, containing 0.10 mol/L NaCl to maintain the ionic strength. HSA at a concentration of 1.0×10^{-5} mol/L and ECH at a concentration of 1.0×10^{-3} mol/L were prepared using the Tris-HCl buffer. VER was prepared at 1.0×10^{-3} mol/L using ethanol.

The instruments used are as follows: F-7000 fluorescence spectrophotometer (Hitachi Co., Japan); UV-2450 UV-Vis spectrophotometer (Shimadzu Corporation, Japan); ZD-2 Precision pH meter (Shanghai Leici Instrument Factory); and SGI O2 computer graphics workstations, DOCK software (version 4.02).

Molecular docking

The VER/ECH molecular structure is shown in fig. 1. All chemical structures were built using the ChemBioOffice ultra software, version 8.0, and then optimized based on the molecular mechanics MM2 force field. The tertiary structures of HSA-VER/ECH complexes were constructed by molecular docking which were using the DOCK 4.02 package and the SGI

work station to conduct molecular docking. The crystal structure of the carrier protein HSA (PDB ID: 1H9Z, 2.5Å) [38] was used as the initial template. Water molecules, cofactors and ligands were removed and explicit hydrogen atoms were added to HAS [28]. AutoDock contains several methods for searching different conformation, among them, the genetic algorithm (GA) provides an effective search for a wide range of applications and was selected for all molecular docking calculations, the parameters were as follows: the random population and substrate conformations of up to 150 arbitrary orientations, a mutation rate of 0.02, and a crossover rate of 0.8. Simulations were carried out considering 2.5 million energy evaluations with a maximum of 27000 generations [28]. finally generating 10 docked conformations. The AutoDock Toolkit was used to optimize the HSA when the molecular docking pretreatment was conducted. To confirm the active site of HSA, the experience potential energy function was used to evaluate the best binding mode of the ligand and a target enzyme [8].

Experimental methods

To measure the fluorescence spectra of VER or ECH with HSA and absorption spectrum of VER or ECH, we pipetted a 2.5 mL HSA solution in a 1 cm quartz cuvette, added 1.0×10^{-3} mol/L VER or ECH solution into the cuvette successively by a micro-injector, and conducted a fluorescence titration (titrant cumulative volume ≤ 100 μL). The buffer solution was used as the fluorescence blank correction. Emission and excitation slit widths were 2.5 nm when measuring the fluorescence signal. The wavelength scan speed was 1200 nm/min, the fixed excitation wavelength was 295 nm, and 250~450 nm emission spectra were plotted at room temperature. The background fluorescence of the buffer was subtracted, and the inner-filter effect was eliminated according to the following equation [29]:

$$F_e = F_m e^{(A_1+A_2)/2} \quad (1)$$

where F_e and F_m are the corrected and measured fluorescence, respectively; A_1 and A_2 are the sum of the absorbance of HSA and ECH/VER at the exciations and max emission wavelengths, respectively.

The synchronous fluorescence spectra of the solution system was scanned by the fluorescence spectrometer at a condition of a fixed difference ($\Delta\lambda$ = 15 nm or $\Delta\lambda$ = 60 nm) between excitation and emission wavelengths [30]. Emission and excitation slit widths were the same as before and the scan speed was 240 nm/min. The Tris-HCl buffer solution was used as the fluorescence blank correction. For the assay of the fluorescence polarization, the excitation wavelength was fixed at 282 nm. Initially, we excited the sample with vertical polarized light and detected the vertical polarization component I_{VV} and the horizontal polarization components I_{VH} of fluorescence. We then excited the sample with horizontal polarized light and detected the vertical polarization component I_{HV} and the horizontal polarization component I_{HH} of the fluorescence. The fluorescence polarization spectra were recorded at room temperature between 250 and 900 nm.

We pipetted 2.5 mL Tris-HCl buffer solution into 1 cm quartz cuvette, added 1.0×10^{-3} mol/L VER or ECH solution to a final concentration of 1.0×10^{-5} mol/L using a micro-injector, and then measured the ultraviolet (UV) absorption spectra between 500 and 190 nm. The scanning speed was at a medium level and the slit width was 2.5 nm. The buffer solution was used as the baseline signal [20, 12].

Results and Discussion

The study of molecular dockings

To determine the interactions of VER/ECH with HSA at the atomic level, the crystal structure of the carrier protein HSA (PDB ID: 1H9Z, 2.5Å) was used as the initial template. Molecular docking has been effectively used for exploring interactions of HSA with various ligands [31, 32, 33]. VER/ECH systems were docked in hydrophobic site II of HSA. The binding models of the molecular docking of VER/ECH to HSA are shown in Fig. 2 and 3.

A

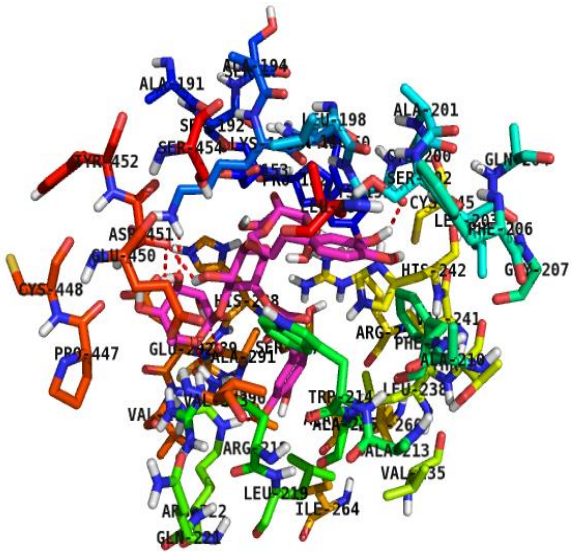

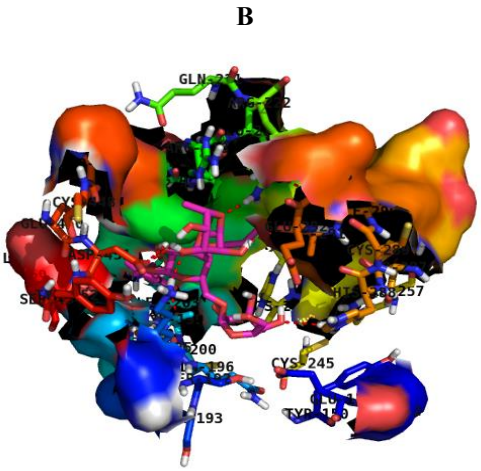

Fig. 2: Interaction mode (A) and hydrophobic surface map (B) between ECH and HSA, only residues around 10.0 Å of the ligand are displayed. The residues of HSA and the ligand structure are represented using stick model, there into red sticks represented oxygen. The hydrogen bond between the ligand and the protein is represented using red dashed line.

Fig. 2 shows the molecular docking diagram (A) and hydrophobic surface diagram (B) of the interaction between VER and HAS, and FIG. 3 shows the molecular docking diagram (A) and hydrophobic surface diagram (B) of ECH interacting with HAS. Fig. 2 shows that VER interacted with HSA at the hydrophobic pocket and that the whole molecule is surrounded by amino acids. VER is in closely binding to the tryptophan residue (Trp214) and phenylalanine residues (Phe206, Phe211) of HSA. Fig. 3 shows that also ECH interacted with HSA at the hydrophobic pocket. This interaction is close to tyrosine (Tyr150 and Tyr452) and phenylalanine (Phe206 and Phe211) residues of HSA. This binding close to aromatic amino acids explains the phenomenon that the fluorescence of HSA were quenched by VER/ECH. Meanwhile, in the binding process of VER to HSA, hydroxyl oxygens, which are vicinal and next to a methyl group in the B ring of VER, form hydrogen bonds with Asp451 and Glu450. The oxygen of the hydroxyl group in the *meta*-position of the D-ring of VER forms a hydrogen bond with His242. In the binding process of ECH to HSA, the oxygen of the *para*-hydroxyl group of the A ring of ECH forms a hydrogen bond with Arg222, whereas the hydrogen forms a hydrogen bond with Ile290. On the B ring, the hydrogen of the *meta*-hydroxyl group forms a hydrogen bond with l291, the oxygen and hydrogen of the *para*-hydroxyl group forms a hydrogen bond with Lys195 and Asp451, respectively. The rationality of the above molecular docking results was verified by the re-docking test and the subsequent fluorescence spectrum verification experiment. The ring oxygen atom of ECH forms a hydrogen bond with Arg222 and the oxygen of the *meta*-hydroxyl group of the D ring forms a hydrogen bond with Arg257. In addition, the hydrogen of the *para*-hydroxyl group of the E ring forms a hydrogen bond with Arg257.

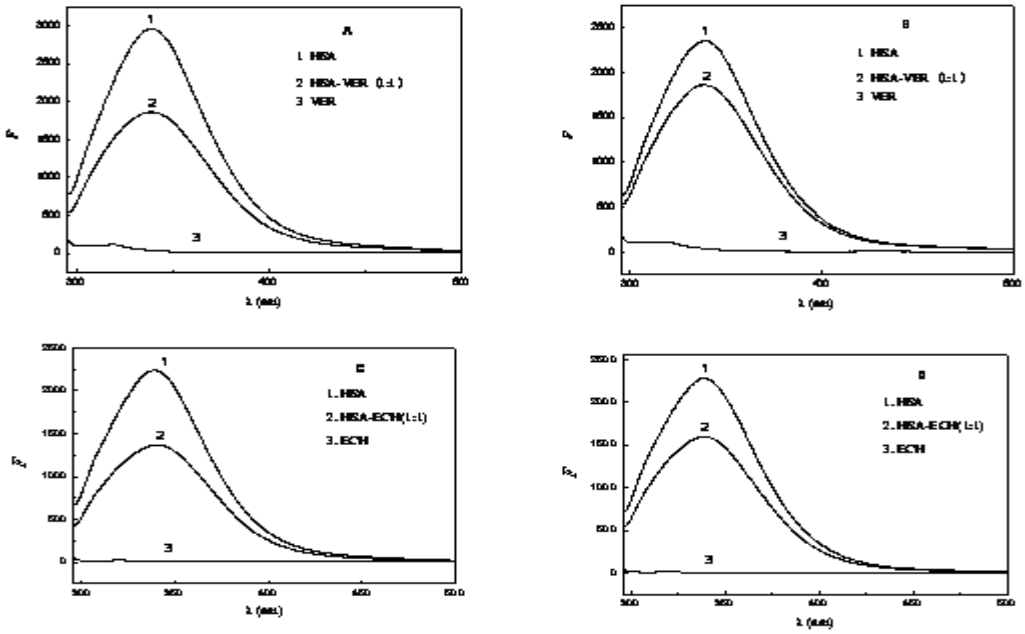

Fig. 3: Fluorescence emission spectra of HSA-ECH/VER solution system.

$c_{(HSA)} = c_{(ECH)} = 1.0\times10^{-5}mol\cdot L^{-1}$

VER and ECH bind non-covalently to the active site of HSA. Around the VER pocket Ala194, Ala201, Ala210, Ala213, Ala215, Ala217, Ala449, Leu198, Leu203, Leu453, Leu457, Leu460, Leu481, Phe206, Phe211, Trp214, Val343, Val344, Val455, Val456, Val482, and Pro447 form a hydrophobic region that indicates that the interactions between VER and the protein are not only hydrogen bonds and van der Waals forces, but also hydrophobic interactions. Around the binding pocket of ECH, residues Leu203, Leu198, Leu219, Leu238, Leu260, Leu481, Ala191, Ala194, Ala201, Ala210, Ala213, Ala215, Ala 261, Ala 291, Phe206, Phe211, Val235, Val241, Val293, Val343, Ile264, Ile290, Pro152, Pro447, and Trp214 form a hydrophobic region. The rationality of the above molecular docking results was verified by the re-docking test and the subsequent fluorescence spectrum verification experiment. From molecular dockings results we know that hydrophobic interactions play a major role. These hydrophobic interactions are the main driving force in the binding of ECH to the protein molecule. By as shown in Fig 2, ECH/VER molecules combine with HSA process, ECH/VER molecules on the benzene ring and Trp214 parallel, resulting π-π interactions formed. [22], resulting π-π interactions formed. The binding of ECH/VER changed the orientation of Trp214, which at least explains the reason of ECH/VER induce the concen tration-dependent fluorescence spectra [22].

Determining the interaction between VER or ECH and HSA

The interaction between drugs and biological macromolecule is usually because of hydrogen bonding, van der Waals interaction, electrostatic interaction forces, or hydrophobic interactions. Within a certain temperature range, ΔH of the interaction process may be regarded as constant. The thermodynamic parameters of the interaction can be calculated. The thermodynamic parameters of the conjugation reaction between VER or ECH and HSA can be calculated by the obtained binding constant K, according to the thermodynamic equations (2), (3), (4) [6] .

$$\Delta G = \Delta H - T\Delta S \quad (2)$$

$$\Delta G = -RT \ln K \quad (3)$$

$$\ln\left(\frac{K_2}{K_1}\right) = \left(\frac{\Delta H}{R}\right)\left(\frac{1}{T_1} - \frac{1}{T_2}\right) \quad (4)$$

The molecular mechanism describing the interaction between the drug and protein is derived from the interaction model [18]. The type of interaction forces between HSA-VER/ECH can be determined as follows [25]: $\Delta S > 0$ represents hydrophobic and electrostatic forces; $\Delta S < 0$ shows hydrogen bonds and van der Waals forces; typical hydrophobic forces when $\Delta H > 0$, $\Delta S > 0$; and hydrogen bonds and van der Waals forces when $\Delta H < 0$, $\Delta S < 0$.

The results in Table 3 show that the $\Delta H < 0$ and $\Delta S < 0$ between HSA and VER. The main interaction involves hydrogen and Van der Waals forces. Those of ECH-HSA are all > 0, and thus their interaction is driven mainly by hydrophobic forces.

In conclusion, we know that the non-covalent interaction between VER and HSA is mainly hydrogen bond, van der Waals force and hydrophobic interaction, while the interaction between ECH and HSA is driven by hydrophobic force.In conclusion, the main forces between VER and HSA are hydrogen bond, van der Waals force and hydrophobic force. To verify the bonding mechanism and bonding forces between VER/ECH and HSA, we confirmed the rationality of the molecular dockings by subsequent spectroscopic experiments. We conducted re-dock verification against the established molecular docking system of HSA-VER/ECH after removing VER/ECH, performed re-docking, and generated a new docking system HSA-RWF (R-warfarin). To verify the reliability of the docking system, we compared the results with the source data in the Protein Data Bank (PDB) created by Brookhaven national laboratory in 1971.The comparison shows that the result is the same.

The fluorescence spectra and binding reaction mechanism of the interaction between VER/ECH and HSA

Fig. 4 shows the fluorescence spectra of VER, ECH, HSA and the mixed systems of VER or ECH and HSA at 25 and 37 °C. At the excitation wavelength of 295 nm, the maximum emission wavelength of HSA is 340 nm, while the maximum emission wavelength of ver-hsa and ech-hsa is about 320 nm, and the maximum emission wavelength of ech-hsa is a little higher than 340 nm. It can be preliminarily determined that the addition of VER causes the conformation change of HSA, while the addition of ECH probably does not cause the conformation change of HSA.This may be due to the structural difference between VER and ECH by a glucosyl ligand. From the fluorescence spectrum of the VER-HSA and ECH-HSA systems, we can conclude that the addition of a drug leads to a reduction in the fluorescence intensity of HSA, indicating that there is an interaction between the drug and HSA and that an energy transfer occurs.

Fig. 5 shows the UV absorption difference spectra of VER-HSA and ECH-HSA. The difference spectrum between VER-HSA and VER is slightly lower compared with the UV absorption curve of HSA, thereby indicating that VER can induce a decrease in the UV absorption of HSA. The differential spectrum between ECH-HSA and ECH is essentially the same as the UV absorption spectrum curve of HSA, which preliminary indicates that ECH has no effect on the UV absorption of HSA. It can be found that the difference spectrum of ver-hsa mixture and VER decreases slightly compared with the ultraviolet absorption curve of HSA, indicating that the ultraviolet absorption of HSA decreases with the addition of VER.The difference spectrum of ECH-HSA mixture and ECH coincides with the uv absorption curve of HSA almost completely, indicating that the addition of ECH has not changed the uv absorption of HSA.It is preliminarily determined that the conformation of HSA has been changed by the addition of VER while that of HSA has not been changed by ECH.This may be due to the structural difference between VER and ECH by a glucosyl ligand.

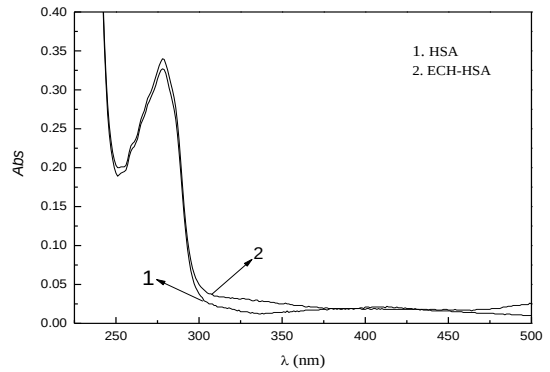

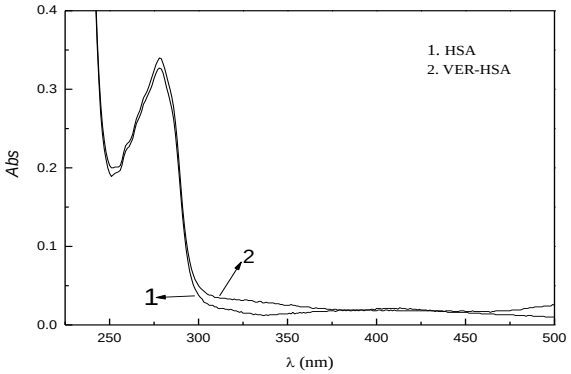

Fig. 4: Absorption difference spectrum of ECH/VER-HAS.
$c_{(HSA)}$=$c_{(ECH)}$= 1.0×10^{-5}mol·L^{-1}

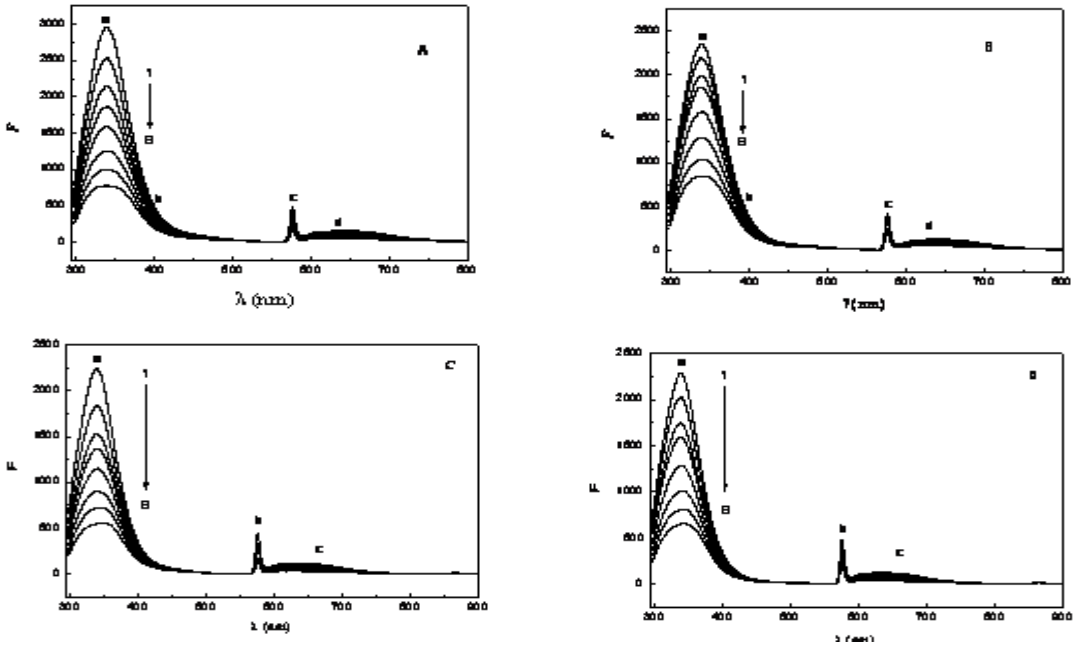

Fig. 5: Fluorescence quenching spectra of HSA interacting with ECH/VER
$c_{(HSA)}$=1.0×10^{-5} mol·L^{-1}, $c_{(ECH)}$/10^{-5}mol·L^{-1},1 to 8: 0.0, 0.4, 0.8, 1.0, 1.6, 2.4, 3.2, 4.0

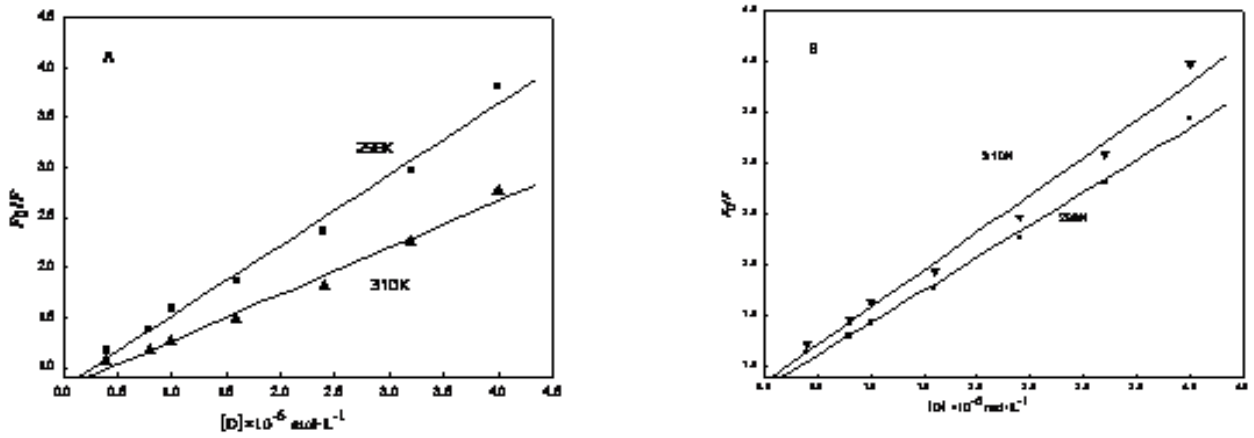

Fig. 6: Stern-Volmer curves of HSA fluorescence quenching by ECH/VER.

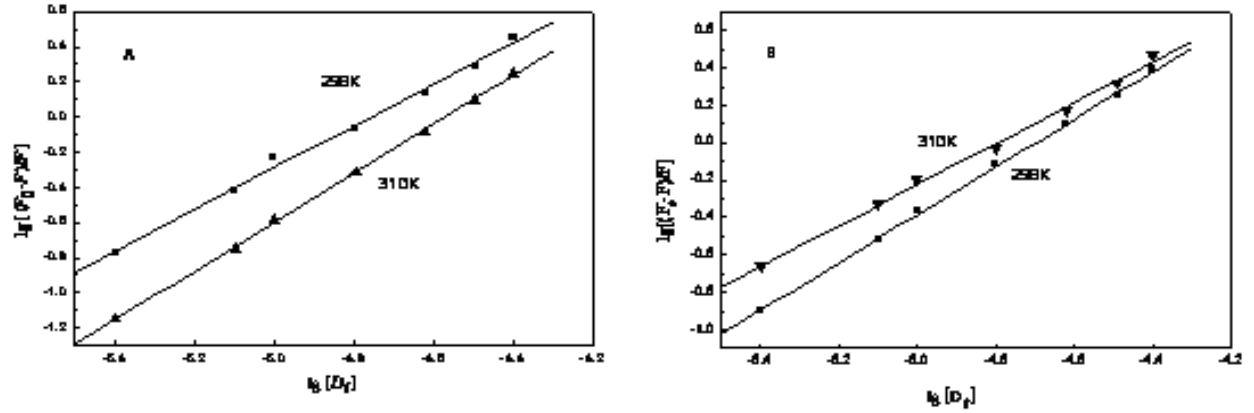

Fig. 7: Fluorescence change linear fitting results of ECH/VER-HSA system
pH=7.40, λ_{ex}=282 *nm*, $c_{(HSA)}$=1.0×10^{-5} mol·L^{-1}, $c_{(ECH)=}$10^{-5} mol·L^{-1}

Fig. 6 shows that changes of the fluorescence emission spectrum of HSA are correlated to the changes in the VER or ECH concentration. Peak *a,* which is the first level of the fluorescent peak of HSA, gradually decreases with the addition of the drug. The peak b is the primary emission peak of ECH/VER and the peak c is the secondary fluorescence frequency doubling peak of Tris-HCl. The intensity of these peaks indicates that VER/ECH has a quenching effect on human serum albumin. The peak d is the Secondary fluorescence frequency doubling peak of the ECH/VER.. When the concentration of HSA was fixed at 1.0 × 10^{-5} mol/L, the fluorescence intensity of HSA was reduced as the concentration of the drug in the system increased from 0 to 4.0 x 10^{-5} mol/L. This shows that VER or ECH can quench the fluorescence signal of HSA.

Fluorescence quenching mechanisms are usually divided into dynamic and static quenching [3]. The dynamic fluorescence quenching can be analyzed by the Stern-Volmer equation [5].To evaluate the interaction mechanism of HSA-VER/ECH system, used the Stern-Volmer equation to analyze the data [29].

$$F_0 / F = 1 + K_q \tau_0 [D] = 1 + K_{SV}[D] \qquad (5)$$

where F_0 and F are fluorescence intensities in absence and presence of ligand, respectively; K_q represents quenching rate constant, L·mol^{-1}·s^{-1}; τ_0 is the average fluorescence lifetime of the HSA without VER/ECH; [D] is the VER/ECH, mol·L^{-1}; K_{sv} is the Stern-Volmer quenching constant, L·mol^{-1} (K_q=K_{SV}/τ_0), *i.e*, the specific value of the quenching rate constant (K_q) may be obtained from the Stern-Volmer quenching constant and the average fluorescence lifetime of the single biomolecule. We measured the fluorescence spectra of the interaction between VER or ECH and HSA. The results obtained are shown in Fig. 7.

Because the average fluorescence lifetime of biological macromolecules is $\tau_0 = 10^{-8}$ s without quencher [21, 10], the quenching constants K_{sv} and K_q of the interaction between VER or ECH and HSA at different temperatures can be calculated by the Stern-Volmer equation based on the experimental data. The calculated data are listed in Table 2.

Table-1: The thermodynamic parameters of ECH binding with HAS.

Solution system	T	ΔH (kJ·mol^{-1})	ΔS (J·mol^{-1}·K^{-1})	ΔG (kJ·mol^{-1})
VER-HSA	298K	-42.29	-34.18	-32.10
	310K			-31.69
ECH-HSA	298K	111.19	473.57	-29.94
	310K			-35.62

Table-2: The quenching constants of ECH to HSA solution system.

Solution system	T	K_{sv}	K_q	R
VER-HSA	298K	8.1330×10^{4}	8.1330×10^{12}	0.9926
	310K	7.9820×10^{4}	7.9820×10^{12}	0.9935
ECH-HSA	298K	8.4735×10^{4}	8.4735×10^{12}	0.9925
	310K	6.3959×10^{4}	6.3959×10^{12}	0.9974

There are currently two commonly used methods to determine the fluorescence quenching mechanism of the interaction of active small molecules with biological macromolecules. One method is to compare the rate constant of the process of bimolecular quenching and the maximum diffusion collisional rate constant of quenching between biological macromolecules and quencher (2.0×10^{10} L·mol^{-1}·s^{-1}) [18, 19]. The second method is to determine the fluorescence quenching mechanism directly by variable temperature experiments [3]. To determine the quenching mechanism of VER or ECH on HSA, we plotted the Stern-Volmer of VER or ECH and HSA at different temperatures (Fig. 7). In Fig. 7, the Stern-Volmer curve of the quenching of HSA fluorescence by VER or ECH exhibits a linear relationship. Within the selected range of concentrations, the quenching constant decreased as the temperature increased. This indicates that the quenching of HSA fluorescence by VER or ECH is static. In Table 2, the bimolecular quenching rate constant K_q values of the experimental system is much larger than 2.0×10^{10} L·mol^{-1}·s^{-1}, indicating that the quenching of HSA fluorescence by VER or ECH is static, which is dominated by the formation of complexes. Thus, the results of the two methods show that the fluorescence quenching mechanism of VER or ECH on HSA is static.

The binding constant (K) and the number of binding sites (n) describing the interaction between VER or ECH and HSA

The dynamic fluorescence quenching mechanism of the interaction between VER or ECH and HSA was obtained from experimental data. The theoretical calculation formula of binding parameters is based on the relationship between the fluorescence intensity of fluorescent molecules and quencher concentration [5]:

$$\lg\left[\frac{F_0 - F}{F}\right] = \lg K + n\lg\left[D_f\right] \qquad (6)$$

where F_0 and F are the relative fluorescence intensities before or after the addition of ligand. K represents is the binding constant and n is the number of binding sites. Because the solution volume of the added VER or ECH is far less than the total volume in the cuvette, it is reasonable to use the total concentration of the quencher [D] instead of [D_f]. The binding parameters were obtained by plotting lg[$(F_0$-$F) / F$] *versus* lg [D] (Fig. 8). The calculated values are shown in Table 3. Fig. 8, in conjunction with Table 3, shows that there exists a strong bonding interaction and a binding site for VER or ECH on HSA. This means that VER or ECH and HSA form a stable complex.

Measuring energy transfer parameters of the VER or ECH and HSA system

According to the Fōrster non-radiative energy transfer mechanism [7, 15], we can obtain the energy transfer efficiency between quencher molecules and protein molecules was obtained. We can also obtain the combined distance between quencher and fluorescence emission residues of a protein. According to this theory, the energy transfer efficiency between fluorescence emitters and fluorescence quencher E has a relationship with the distance between the two (r) and the critical energy transfer distance R_0:

$$E = \frac{R_0^{\,6}}{R_0^{\,6} + r^6} \qquad (7)$$

where E represents the energy transfer efficiency; R_0 represents the critical energy distance when the energy transfer efficiency E = 50%.

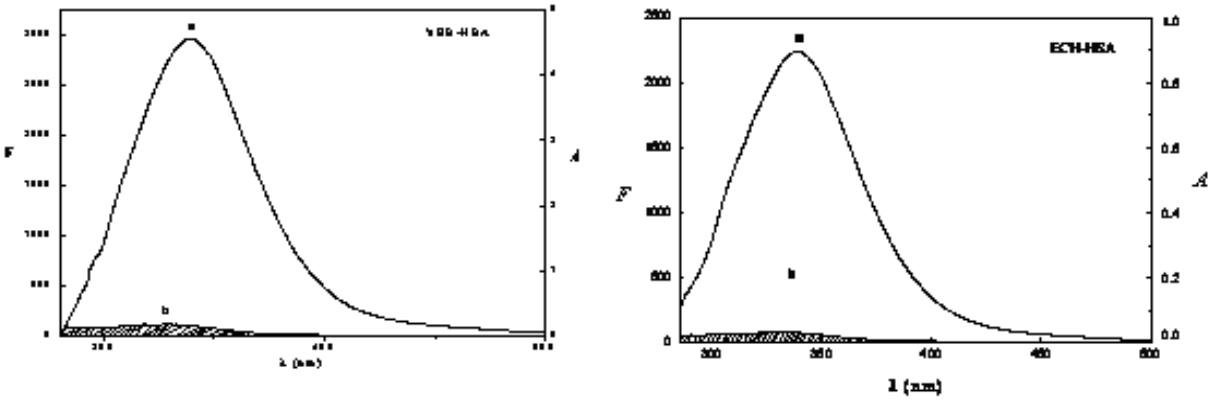

Fig. 8: Overlap between the fluorescence emission spectra of HSA (a) and UV absorption spectra of ECH/VER.

Table-3: The binding parameters of ECH to HAS.

Solution system	*K*	(L·mol^{-1})	*n* (结合位点数)	拟合方程	*R*	(相关系数)	*SD*	*P*
VER-HSA(298K)		4. 2403×10^5	1.18	*y*=5.6247+1.1827 *x*		0.9973	0.0343	<0.0001
VER-HSA(310K)		2.1900×10^5	1.39	*y*=6.3404+1.3878 *x*		0.9997	0.0133	<0.0001
ECH-HSA(298K)		1.7710×10^5	1.09	*y*=5.2482+1.0943 *x*		0.9982	0.0256	<0.0001
ECH-HSA(310K)		1.0061×10^5	1.28	*y*=6.0027+1.2774 *x*		0.9997	0.0121	<0.0001

$$R_0^{\ 6} = 8.8\times10^{-25} K^2 N^{-4} \Phi J \qquad (8)$$

where K^2 is the dipole spatial orientation factor, N is the refractive index of media, Φ is the optical quantum efficiency of protein molecules, and J is the spectral overlap integral between fluorescence emission spectra of protein molecules and the absorption spectra of the drug, cm^3·L·mol^{-1}.

$$J = \int_0^\infty F(\lambda)\varepsilon(\lambda)\lambda^4 \mathrm{d}\lambda / \int_0^\infty F(\lambda)d\lambda \qquad (9)$$

where $F(\lambda)$ represents the fluorescence intensity of the protein molecule at a wavelength λ and $\varepsilon(\lambda)$ is the molar absorption coefficient of a drug at wavelength λ, L·mol·cm^{-1}.

The energy transfer efficiency E can be measured according to the following formula:

$$E = 1 - F / F_0 \qquad (10)$$

A plot superimposing the obtained UV spectra and fluorescence spectra is shown in Fig 9.

Fig. 9 shows that the fluorescence spectrum of HSA partially overlaps with UV absorption spectrum of VER or ECH.The dipole-dipole non-radiative energy transfer theory of Förster the phenomenon of non-radiation energy transfer will occur between the excited energy body molecules and juxtapositioned receiving body molecules [16], when the two bodies are close enough (the distance between them must be less than 7 nm). When the fluorescence emission spectrum overlaps with the absorption spectrum of the receiving body, the fluorescence of the energy body will be quenched. The combined distance between the energy and receiving bodies can be obtained by this relationship. The calculated spectral overlap integral of the binding reaction of HSA-VER or HSA-ECH is J = 1.81/1.67×10^{-14} cm^3·L·mol^{-1} according to equation (8), and the energy transfer efficiency is E = 0.46/0.31 according to equation (9). Under the conditions of this experiment, taking the dipole spatial orientation factor as the mean of the random distribution of two conjugates, *i.e.*, K^2 = 2/3, the photoluminescence efficiency for tryptophan of Φ = 0.118, the refractive index N = 1.336, and substitution of the above equation into (11) and (6), the critical energy distance of HSA and the combined distance were obtained: R_0 = 2.72 and 2.68 nm and r is 2.79 and 2.75 nm for VER-HSA and ECH-HSA, respectively. Since r < 7 nm we can conclude that non-radiation energy transfer to VER or ECH occurs, which causes fluorescence quenching of HSA.

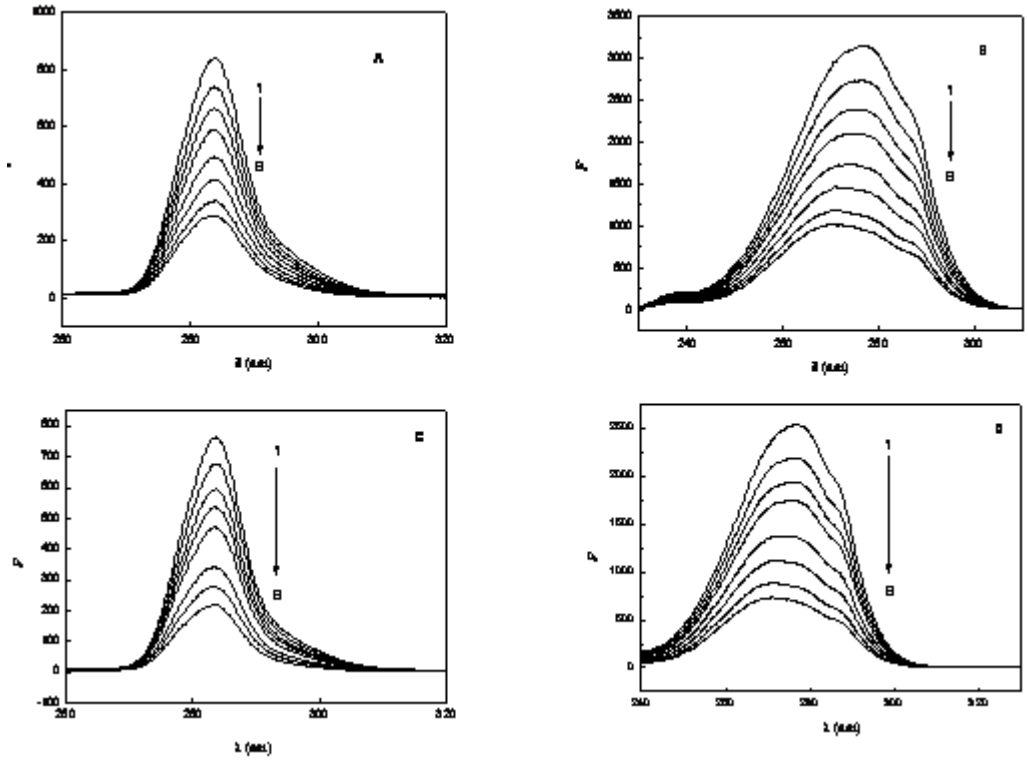

Fig. 9: Effect of the ECH/VER on the synchronous fluorescence spectrum of HSA

The influence of VER or ECH on the conformation of HSA

In the synchronous fluorescence spectra of a protein, the fluorescence spectral characteristics of tyrosine residues are displayed when $\Delta\lambda$ = 15 nm and the fluorescence spectral characteristics of tryptophan residues are also displayed when $\Delta\lambda$ = 60 nm. The maximum emission wavelength of amino acids of proteins is related to the polarity of its environment, so a change in the protein conformation can be judged by the maximum emission wavelength [23]. By fixing the concentration of HSA and increasing the concentration of VER or ECH, we can obtain the synchronous fluorescence spectra of the VER-HSA or ECH-HSA system (Fig 10).

Fig 10 shows that the fluorescence of HSA is mainly contributed by tryptophan. As the drug concentration increased, the maximum emission wavelength of the tyrosine residue remained unchanged (Fig. 10 A, C). When $\Delta\lambda$ = 60 nm, the maximum emission wavelength of tryptophan residues is red shifted. There is a shoulder at 287 nm in Figs 10 B and D. This shoulder arises from VER or ECH and not from the protein. The red shift indicates that the binding of VER or ECH to HSA causes a change in the conformation of HSA and affects the micro-environment where the tryptophan residues of HSA reside. This means that the hydrophobic forces of the binding have been reduced. The part of peptide chain that makes up the hydrophobic cavity is dynamic, thus contributing to the subtle conformational changes to HSA.

The influence of the binding reaction of VER-HSA and ECH-HSA on the conformational change of HSA

To further understand the kinetic mechanism of the binding reaction of VER or ECH to HSA on the conformational change to HSA, the fluorescence phase diagrams required further analysis. The fluorescence phase diagrams describe the change in protein structure after measuring the change in fluorescence intensity $I(\lambda_1)$ and $I(\lambda_2)$ of the protein at the emission wavelengths λ_1 and λ_2. The fluorescence intensity is a breadth of nature and therefore the following relationship exists [17] :

$$I(\lambda_1) = a + bI(\lambda_2) \tag{11}$$

$$a = I_1(\lambda_1)I_1(\lambda_2(I_2(\lambda_1) - I_1(\lambda_1))/(I_2(\lambda_2) - I_1(\lambda_1)) \tag{12}$$

$$b = (I_2(\lambda_1) - I_1(\lambda_1))/(I_2(\lambda_2) - I_1(\lambda_2)) \tag{13}$$

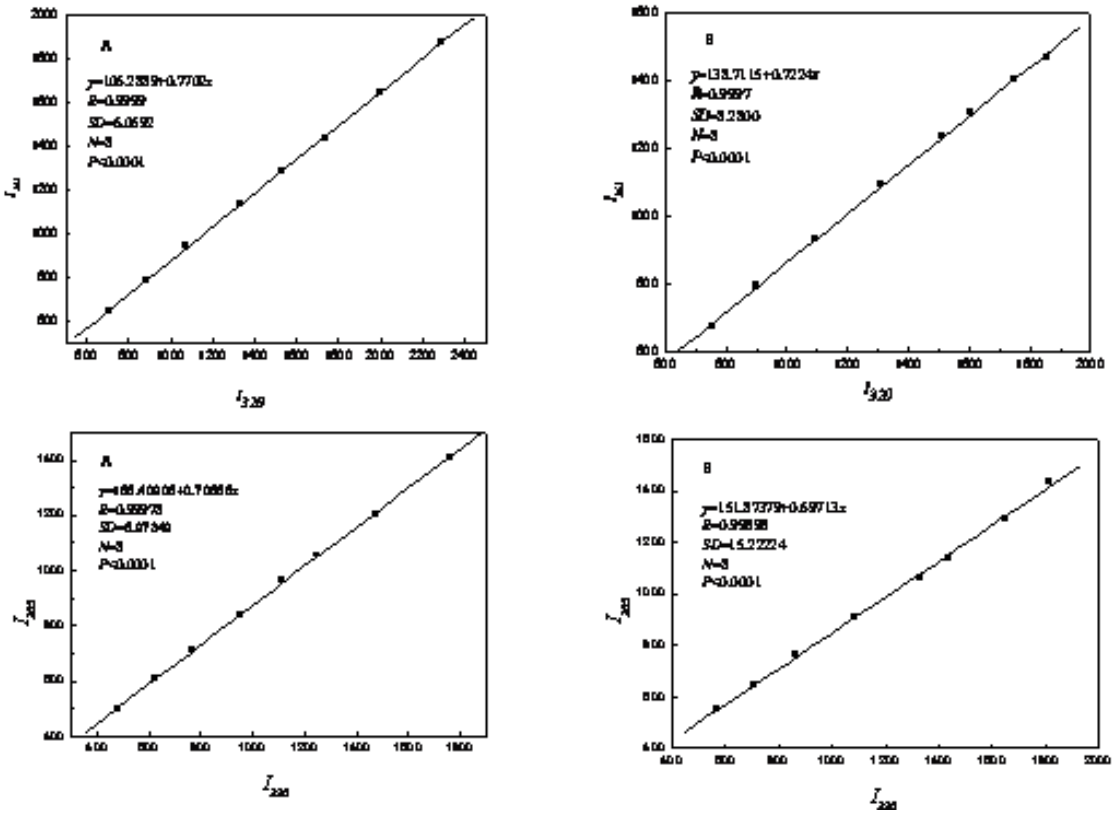

Fig. 10: The fluorescence phase diagrams of ECH-HSA system (A: 25℃; B: 37℃)

In the equation, $I(\lambda_1)$ and $I(\lambda_2)$ are the measured fluorescence intensities when the emission wavelengths are λ_1 and λ_2 under different experimental conditions. If the experimental data plotted according to equation 10 is linear, the corresponding change in the protein conformation obeys a "two-state" model. Conversely, if the relation is non-linear the transition process of the protein conformation is an order change process. If the relationship shows two or more straight lines, and each of which describes an "all or nothing" process of structural changes to the protein, then it meets the "multi-state model".

The phase diagram result of I_{320}–I_{365} is the most accurate in this experiment. Fig 11 is the corresponding fluorescence phase diagram that is prepared according to the experimental data. As can be seen from Fig 11, the fluorescent phase diagrams of the binding reaction of VER or ECH and HSA are linear. This indicates that when VER or ECH is non-covalently bound to HSA, the process of change to the conformation of HSA is a "two-state" model.

The influence of VER or ECH on the tryptophan microenvironment HSA

A polarized fluorescence spectrum could quantitatively reflects the interaction between VER/ECH and HSA. The polarized fluorescence spectrum can be obtained by the degree of polarization (*P*) and the anisotropy (*r*) where in the degree of polarization *P* can be calculated according to the following formula:

$$P = (I_W - GI_{VH})/(I_{VV} + GI_{VH}) \quad (14)$$

where *G* is a correction factor ($G = \frac{I_{HV}}{I_{HH}}$). I_{VV} and I_{VH} are the intensity of emitted light of the vertical polarized perpendicular and horizontal polarized perpendicular excited by vertical polarized light, respectively. I_{HV} and I_{HH} are the intensity of emitted light of the vertical polarized perpendicular and the horizontal polarized perpendicular excited by horizontal polarized light, respectively. The anisotropy, *r*, can be calculated as follows.

$$\mathrm{r} = \frac{I_{VV} - I_{VH} \times G}{I_{VV} + 2I_{VH} \times G} \quad (15)$$

After addition of different concentrations of VER or ECH to a fixed concentration of HSA, we recorded fluorescence polarization data and then calculated *P* and *r* according to equations (11) and (12). The results are shown in Table 4.

Table-4: The fluorescence polarization parameters of ECH-HSA systems.

Solution system	I_{VV}	I_{VH}	I_{HV}	I_{HH}	*G*	*P*	*r*
HSA	**204.6000**	**152.5000**	**121.5000**	**112.8000**	**1.0771**	**0.1094**	**0.0757**
VER-HSA	**144.6000**	**107.6000**	**86.1600**	**80.2400**	**1.0738**	**0.1117**	**0.0774**
ECH-HSA	**116.3000**	**87.1000**	**68.3100**	**63.8100**	**1.0705**	**0.1100**	**0.0762**

The degree of polarization of the fluorophore and anisotropy is inversely proportional to the rotational speed of the fluorophore. The smaller the fluorophore is, the faster the rotational speed and the smaller the degree of polarization and anisotropy. The data presented in Table 4 show that the rotational speed of the fluorescent molecule HSA is fast in aqueous phase, that depolarization is large, and that the degree of polarization and anisotropy are small. After the interaction of HSA with VER or ECH, the degree of polarization and anisotropy of HSA increased, confirming that there exist intermolecular interactions between the drug and the protein molecules. After the formation of a complex, the volume of the fluorophor (HSA) is increased, the molecular rotation is hindered, and the rotation speed is reduced. The viscosity of the system becomes higher and thus, the degree of fluorescence polarization also becomes higher. The experimental data quantifiably proved that there exist interactions between HSA and VER or ECH and that they form non-covalent complexes. The degree of polarization and anisotropy of HSA increased more when VER was added to the protein sample compared to the addition of ECH. This indicates that the complex between VER and HSA is stronger than between ECH and HSA. In addition, VER binds to HSA easier than ECH. This difference in binding is most likely due to the relatively smaller size of VER and its lower polarity.

Conclusion

This report studied the interaction between active ingredients of traditional Chinese medicine VER or ECH and HSA using spectroscopic methods combined with molecular modeling. Molecular modeling revealed the binding sites of the drug on HSA and thermodynamic functions were obtained by the integrated experiments. The results indicated that the interplay between VER and HSA primarily involves hydrogen bonds and van der Waals forces, whereas the interaction between ECH and HSA involves mainly hydrophobic forces. The spectroscopic results showed that the reaction mechanism between drug molecules and HSA is static quenching. According to the theory of energy transfer,Non-radiative energy transfer took place. The binding of VER or ECH leads to changes in the conformation of HSA and the changes are consistent with a “two-state” model. According to the analysis of fluorescence polarization, HSA shows an interaction with the drug and forms non-covalent complexes. The results are consistent with the computer simulations. This work offers useful results for carrying out further studies on active ingredients of traditional Chinese medicine VER or ECH and HSA. Moreover, the results provide reference values for future research studying the interaction between ECH and its hydrolysis compound, VER, with proteins.

Acknowledgments

This work was supported by the National Natural Science Foundation of China (grant number 20877072), the Natural Science Foundation of Zhejiang Province (No. LY14E030016), and the found of the Key Laboratory of Chemical Utilization of Forestry Biomass of Zhejiang Province.

Conflicts of Interest

The authors declare no conflict of interest.

References

1. L. D. Bertozo, E. A. Philot, A. N. Lima, P. T. D. Lara and A. L. Scott, Ximenes VF Interaction between1 pyrenesulfonic acid and albumin: Moving inside for the protein, *Pergamon-Elsevier Science Ltd.*, **208**, 243 (2018).
2. B. L. Bian, J. H. Wang and J. Yang, The comparison of verbascoside content in five different organs. *Chin. J. Chin. Mater. Med*., **35**, 739 (2010).
3. W. Bian, Y. L. Wei and Y.P. Wang, Fluorescence study interaction between caffeine and theophylline and bovine serum albumin. *Spectrosc. Spect. Anal.*, **26**, 505 (2006).
4. W. N. Chen, F. Li, P. P. Zhu, C. F. Zhang and Z. L. Yang, Effects of acteoside on proliferation and differentiation in osteoblasts in vitro. *J. Strait Pharm.*, **24**, 23 (2012).
5. R. Clara, A. Susana and F. Elisabet, Molecular interactions between warfarin and human (HSA) or bovine (BSA) serum albumin evaluated by isothermal titration calorimetry (ITC), fluorescence spectrometry (FS) and frontal analysis capillary electrophoresis (FA/CE). *Journal of Pharmaceutical and Biomedical*

Analysis., **150**, 452 (2018).
6. E. Christopher and B. Dorothy, A Large Solvent Isotope Effect on Protein Association Thermodynamics. *Biochemistry.*, **52**, 6595 (2014).
7. T. Forster, *Modern Quantum Chemistry*. Academic Press, New York, p. 13 (1965).
8. M. Guo, X. M. Wang, X. W. Lu,H. Z. Wang and E. B. Peter, α-Mangostin Extraction from the Native Mangosteen (Garcinia mangostana L.) and the Binding Mechanisms of α-Mangostin to HSA or TRF, *Plos One*., **11**, (2016)
9. O. A. A. Hamdi, S. R. Feroz , J. A. Shilpi, E. H. Anouar, A. K. Mukarram, S. B. Mohamad, S. Tayyab and K. Awang, Spectrofluorometric and molecular docking studies on the binding of curcumenone to human serum albumin. *Internat. J. Mol. Sci*., **16,** 5180 (2015).
10. H. Y. He, Y. Li, H. Z. Si, Y. M. Dong, F. L. Sheng, X. J. Yao and Z. D. Hu, Molecular modeling and spectroscopic studies on the binding of guaiacol to human serum albumin. *J. Photochem. Photobiol. A: Chem*., **182**, 158 (2006).
11. Raphael Bar-Or, Dehydroalanine derived from cysteine is a common post-translational modification in human serum albumin, *Rapid Communications in Mass Spectrometry.*, **22**, 711 (2008).
12. Y. J. Hu, H. L. Yue, X. L. Li, S. S Zhang, E. Tang and L. P. Zhang, Molecular spectroscopic studies on the interaction of morin with bovine serum albumin. *J. Photochem. Photobiol. B: Biol*., **4**, 16 (2012).
13. D. P. Yeggoni, A. Rachamallu and R. Subramanyam, Protein stability, conformational change and binding mechanism of human serum albumin upon binding of embelin and its role in disease control, *Journal of Photochemistry and Photobiology B: Biology.*, **160**, 248 (2016)
14. C. H. Li, J. H. Liu, Z. X. Xu, W. Zhao, X. Q. Zhang, T. T. Zhang and Z. G. Ma, RP-HPLC simultaneous determination of four phenylethanoid glycosides in *Cistanche tubulosa* (Schrenk) wight. *J. Pharm. Anal.*, **30**, 1003 (2010).
15. H. Lin, J. F. Lan, M. Guan and F. L. Sheng and H. X. Zhang, Spectroscopic investigation of interaction between mangiferin and bovine serum albumin, *Spectrochim. Acta A Mol. Biomol. Spectrosc*., **73**, 936 (2009) .
16. K. C. Oliver, M. D. Patricia and N. W. Daniel, Single molecule fluorescence for membrane proteins. *Methods*., **147**, 221 (2018).
17. N. Rajendiran and J. Thulasidhasan, Interaction of sulfanilamide and sulfamethoxazole with bovine serum albumin and adenine: spectroscopic and molecular docking investigations, *Spectrochim Acta. Part A: Mol. Biomol. Spectroscop.*, **144**, 183 (2015).
18. M. Sasmal, L. A. Roy and T. K. Bhattacharyya, Low-field transport in bovine serum albumin conjugated zno nanoparticle networks. *Ieee Electron Device Letters* **37**, 100 (2016).
19. N. Shahabadi, A. Khorshidi and N. H. Moghadam, Study on the interaction of the epilepsy drug, zonisamide with human serum albumin (HSA) by spectroscopic and molecular docking techniques, Spectrochim. *Acta A Mol. Biomol. Spectrosc***., 114**, 627 (2013).
20. Y. Q. Wang, B. P. Tang, H. M. Zhang, Q. H. Zhou and G. C. Zhang, Studies on the interaction between imidacloprid and human serum albumin: Spectroscopic approach. *J. Photochem. Photobiol. B: Biol*., **94**, 183 (2009).
21. J. G. Xu and Z. B. Wang, *Fluorescence Analytical Method. 3rd ed*, Science Press, Beijing, p. 21 (2006).
22. S. L. Zhuang, H. F. Wang, K. K. Ding,J. Y. Wang, L. M. Pan, Y. L. Lu, Q. J. Liu and C. L. Zhang, Interactions of benzotriazole UV stabilizers with human serum albumin: Atomic insights revealed by biosensors, spectroscopies and molecular dynamics simulations, *Chemosphere*., **144,** 1050 (2016).
23. K. Yutaka and C. D. Hu, Bimolecular Fluorescence Complementation (BiFC) Analysis of Protein-Protein Interaction: How to Calculate Signal-to-Noise Ratio. *Laboratory Methods in Cell Biology: Imaging*., **113**, 107 (2012).
24. S. Y. Zhao, X. Liu, Q. Ji, W. T. Xiong, X. L. Tian, Cao H, Gu L and Liu XZ., A production method of monomeric compound of verbascoside. Patent-101629198 (2011).
25. R. Punith, A. H. Hegde and S. Jaldappagari, Binding of an Anti-inflammatory Drug Lornoxicam with Blood Proteins: Insights from Spectroscopic Investigations, *Journal of Fluorescence***., 21**, 487 (2010).
26. Q. Zhang, H. Yu, F. Z. Zhang and Z. C. Shen, Expression and purification of recombinant human serum albumin from selectively terminable transgenic rice[J]. *Journal of Zhejiang University-Science B(Biomedicine & Biotechnology)*., **14,** 867 (2013).
27. M. Zhong, H. Chen, Y. Jiang, P. F. Tu, C. L. Liu, W. X. Zhang, J. Y. Ma and H. Ding, Effects of echinacoside on striatal extracellular levels of amino acid neurotransmitter in cerebral ischemia rats. *Chin. Pharmacol. Bull*., **28**, 361 (2012).
28. Martínez-Sotres, Carmen, G. José, Rutiaga-Quiñones, H. B. Rafael, M. Gallo and L. A .Pablo, Molecular docking insights into the inhibition of laccase activity by medicarpin, *Wood Science and Technology.*, **49,** 857 (2015).

29. M. Guo, X. W. Lu, Y. Wang and E. B. Peter, Comparison of the interaction between lactoferrin and isomeric drugs, *Spectrochimica Acta Part A: Molecular and Biomolecular Spectroscopy.*, **173**, 593 (2017).
30. Zheng YY, Sun N, Xu MH, Lu YJ, Qiu B, Cheng MJ, Wong WL, Chow CF. Molecular Interaction Kinetics and Mechanism Study of Phytohormones and Plant Protein with Fluorescence and Synchronous Fluorescence Techniques. Chemistryselect**., 2**, 3993-4000, (2017).
31. Gan RX, Zhao LD, Sun QM, Tang PX, Zhang SS, Yang HQ, He JW, Li H, Binding behavior of trelagliptin and human serum albumin: Molecular docking, dynamical simulation, and multi-spectroscopy. *Spectrochimica acta part a-Molecular and Biomolecular Spectroscopy,.* **202**, 187-95, (2018).
32. Hadichegeni S, Goliaei B, Taghizadeh M, Davoodmanesh S, Taghavi F, Hashemi M, Characterization of the interaction between human serum albumin and diazinon via spectroscopic and molecular docking methods. *Human & Experimental Toxicology***., 37**, 959-971, (2018).
33. Liu JM, Yan XY, Yue YY, Zhao SF, Investigation of the interaction of aurantio-obtusin with human serum albumin by spectroscopic and molecular docking methods. *Luminescence.,* **33**, 104-111, (2018).
34. Caufin S, Navarra C, Riva S, Danieli B, Enzymatic acylation as an efficient tool for an easy access to specific acyl derivatives of the natural antioxidants verbascoside, teupolioside and echinacoside. Journal of Molecular Catalysis b-enzymatic.,**104,** 42-47, (2014).
35. Tanino T, Nagai N, Funakami Y, Phloridzin-sensitive transport of echinacoside and acteoside and altered intestinal absorption route after application of Cistanche tubulosa extract. Journal of Pharmacy and Pharmacology., **67**, 1457-1465, (2015).
36. Xie J, Tan F, Zhu J, Yue CB, Li Q, Separation, purification and quantification of verbascoside from Penstemon barbatus (Cav.) Roth. Food Chemistry. **135**, 2536-2541, (2012).
37. Wang XH, Wang XG, Guo YH, Rapidly Simultaneous Determination of Six Effective Components in Cistanche tubulosa by Near Infrared Spectroscopy. Molecules. **22**, (2017).
38. Petitpas I, Bhattacharya A A, Twine S, East M, Curry S, Crystal Structure Analysis of Warfarin Binding to Human Serum Albumin: Anatomy of Drug Site I. J.Biol.Chem. **276**, 22804, (2001).